Received: 2 April 2019 | Revised: 9 December 2019 | Accepted: 12 December 2019

DOI: 10.1111/tbj.13739

ORIGINAL ARTICLE

The Breast Journal WILEY

Digital breast tomosynthesis and contrast-enhanced dual-energy digital mammography alone and in combination compared to 2D digital synthetized mammography and MR imaging in breast cancer detection and classification

Antonella Petrillo MD[1] | Roberta Fusco Eng[1] | Paolo Vallone MD[1] | Salvatore Filice MD[1] | Vincenza Granata MD[1] | Teresa Petrosino MD[1] | Maria Rosaria Rubulotta MD[1] | Sergio Venanzio Setola MD[1] | Mauro Mattace Raso MD[1] | Francesca Maio MD[2] | Concetta Raiano MD[1] | Claudio Siani MD[3] | Maurizio Di Bonito MD[4] | Gerardo Botti MD[5]

[1]Radiology Division, Istituto Nazionale Tumori IRCCS Fondazione G. Pascale, Naples, Italy

[2]Radiology Division, "Universita' Degli Studi di Napoli Federico II", Naples, Italy

[3]Senology Surgical Division, Istituto Nazionale Tumori IRCCS Fondazione G. Pascale, Naples, Italy

[4]Pathology Division, Istituto Nazionale Tumori IRCCS Fondazione G. Pascale, Naples, Italy

[5]Scientific Director, Istituto Nazionale Tumori IRCCS Fondazione G. Pascale, Naples, Italy

Correspondence
Roberta Fusco, Radiology Division, Istituto Nazionale Tumori Fondazione G. Pascale, Napoli, Italia", Via Mariano Semmola, Naples, Italy.
Email: r.fusco@istitutotumori.na.it

Abstract

To compare diagnostic performance of contrast-enhanced dual-energy digital mammography (CEDM) and digital breast tomosynthesis (DBT) alone and in combination compared to 2D digital mammography (MX) and dynamic contrast-enhanced MRI (DCE-MRI) in women with breast lesions. We enrolled 100 consecutive patients with breast lesions (BIRADS 3-5 at imaging or clinically suspicious). CEDM, DBT, and DCE-MRI 2D were acquired. Synthetized MX was obtained by DBT. A total of 134 lesions were investigated on 111 breasts of 100 enrolled patients: 53 were histopathologically proven as benign and 81 as malignant. Nonparametric statistics and receiver operating characteristic (ROC) curve were performed. Two-dimensional synthetized MX showed an area under ROC curve (AUC) of 0.764 (sensitivity 65%, specificity 80%), while AUC was of 0.845 (sensitivity 80%, specificity 82%) for DBT, of 0.879 (sensitivity 82%, specificity 80%) for CEDM, and of 0.892 (sensitivity 91%, specificity 84%) for CE-MRI. DCE-MRI determined an AUC of 0.934 (sensitivity 96%, specificity 88%). Combined CEDM with DBT findings, we obtained an AUC of 0.890 (sensitivity 89%, specificity 74%). A difference statistically significant was observed only between DCE-MRI and CEDM (P = .03). DBT, CEDM, CEDM combined to tomosynthesis, and DCE-MRI had a high ability to identify multifocal and bilateral lesions with a detection rate of 77%, 85%, 91%, and 95% respectively, while 2D synthetized MX had a detection rate for multifocal lesions of 56%. DBT and CEDM have superior diagnostic accuracy of 2D synthetized MX to identify and classify breast lesions, and CEDM combined with DBT has better diagnostic performance compared with DBT alone. The best results in terms of diagnostic performance were obtained by DCE-MRI. Dynamic information obtained by time-intensity curve including entire phase of contrast agent uptake allows a better detection and classification of breast lesions.

KEYWORDS
breast cancer, CEDM, diagnostic accuracy, mammography, tomosynthesis

1 | INTRODUCTION

Mammography (MX) is the standard of care in the detection of breast cancer in screening programs and in symptomatic women. Nevertheless, mammography suffers from several limitations, primarily due to reduced contrast between tumors and surrounding tissue. Especially in dense breasts, this can lead to a decrease in sensitivity and additional imaging methods are necessary.[1] Thanks to the implementation of digital mammography, additional diagnostic accuracy can be achieved for specific subgroups of women, presumably from its superior ability to depict cancers in dense breast tissue.[2] However, MX is an imperfect tool in detecting breast cancer, with an overall sensitivity of 75%-85%, dropping as low as 30%-50% in women with a BRCA gene mutation.[3,4] Specificity is limited, and the positive predictive value of a biopsy recommendation is in the 25%-45% range.[5] As many as 20%-30% of breast cancers will not be detected on a mammogram.[3-5] Mammographic sensitivity decreases with the increasing of parenchyma density[6,7] due to a superimposition of dense breast tissue on a two-dimensional (2D) mammographic projection. As reported in TOMMY trial,[8] sensibility and specificity cancer detection rate in breast tissue, especially in the dense one (>50%), increase with the association of MX with digital breast tomosynthesis (DBT). Moreover, OTST[9] and STORM[10] trials reported that DBT can potentially reduce, also, false-positive recall rates.

DBT is a mammographic technique that permits individual planes of the breast to be visualized while reducing the impact from overlapping tissue.[11] Unlike conventional digital MX, in which each image is created from a single x-ray exposure, tomosynthesis images are reconstructed from a series of low-dose exposures as the x-ray source moves in an arc or linear trajectory above the breast. The resultant imaging data set minimizes the effect of overlapping structures, affording DBT the potential to enhance both the sensitivity and the specificity of radiologic imaging.

For breast cancer staging, MX sensitivity may be even poorer, with missed multifocal or multicentric disease, resulting in incorrect treatment options offered to the patient. Better depiction is possible with breast magnetic resonance imaging (MRI). This is due to its ability to map the abnormal blood flow related to neovascularity associated with breast cancer. The sensitivity of MRI for the depiction of breast carcinoma has been reported in the 79%-98% range.[12-14] MRI is the most accurate method for determining the size of an invasive breast cancer, although it may somehow overestimate the true extent of a ductal carcinoma in situ (DCIS).[15] A meta-analysis of 19 studies showed that MRI depicts mammographically occult multicentric or multifocal disease in 16% of patients.[16] The additional findings led to management changes in 10%-20% of patients,[17,18] particularly in women with tumors larger than 4 cm, lobular cancers, and dense breast tissue.[19] Although breast MR imaging is extremely sensitive, specificity is limited, leading to additional workups and benign-resulting biopsies. Additionally, good quality breast MRI is expensive, time-consuming, and not universally available. Patients with pacemakers, certain aneurysm clips or other metallic hardware, allergy to contrast agents, or severe claustrophobia are unable to undergo MRI.

The development of dual-energy, contrast-enhanced digital MX has made the clinical use of contrast with mammography a possibility. Contrasted-enhanced dual-energy digital MX (CEDM) was approved by the FDA in 2011. It employs dual energy for mammographic acquisition after IV injection of iodinated contrast agent. Previous studies have compared the sensitivity of CEDM to that of conventional digital MX, US, and MRI.[20,21] CEDM sensitivity has been reported high also near to 100% (range 90%-100%),[21,22] being significantly higher compared to MX and US alone. CEDM has been proven to detect additional mammographically occult cancers, to depict more accurately the extent of disease, and to help guide surgical and treatment planning.[23,24] However, few studies have been published on CEDM compared to MRI for breast cancer detection, lesion size estimation, and preoperative staging.[22]

The purpose of this single cancer center study was to prospectively compare the diagnostic performance of CEDM and DBT alone and in combination compared to 2D digital MX and to MRI in women with breast lesions to identify and classify the disease.

2 | METHODS

2.1 | Patient characteristics

Local institutional review board approved the protocol (Deliberation N. 617 of 09/08/2016 of National Cancer Institute of Naples Pascale Foundation). Informed consent was obtained from all patients. The study was performed in accordance with the current version of the Declaration of Helsinki and the International Conference on Harmonization of Good Clinical Practice Guidelines.

TABLE 1 Breast lesion histological type

Benign lesions (N. 53)	Number	%
Adenosis	6	11 321
Dysplasia	7	13 208
Ductal hyperplasia	14	26 415
Fibroadenoma	16	30 189
Fibrosis	9	16 981
Phyllodes tumor	1	1887
Malignant lesions (N. 81)	Number	%
DCIS	16	19 753
IDC	40	49 383
ILC	16	19 753
ITC	11	13 580

TABLE 2 Overview of patient groups for imaging modality

	AUC	Sensitivity	Specificity	PPV	NPV	Accuracy	*P* value
2D BIRADS	0.758	0.660	0.824	0.850	0.615	0.725	.045
DBT BIRADS	0.868	0.835	0.838	0.887	0.770	0.836	.038
CEDM BIRADS	0.883	0.874	0.809	0.874	0.809	0.848	.036
CEDM + 3D BIRADS	0.905	0.932	0.765	0.857	0.881	0.865	.037

Patients were considered eligible when they showed suspicious breast lesions at clinical examination and/or evaluated as BIRADS 3, 4, or 5 (ACR BIRADS® Atlas Fifth Edition) at mammography and/or US, scheduled for fine-needle aspiration cytology or core biopsy. Exclusion criteria were as follows: presence of pacemaker or other devices in the chest wall, inability to keep upright immobility during the examination, internal/external devices preventing from correct patient positioning, pregnancy or breast-feeding, and presence of breast tattoos; nonremovable drilling at the nipple; and breast implants. All patients underwent CEDM and DBT. Two-dimensional synthetized MX images were obtained by DBT. In a 21-month period, we enrolled 100 consecutive patients with breast lesions; their age ranges from 42 to 80 years (median, 58; standard deviation 10.2). One hundred and thirty-four breast lesions subjected to CEDM and DBT were analyzed: 53 histopathologically proven benign lesions and 81 histopathologically proven malignant lesions (see Table 1). A smaller group of patients (n. 70) was subjected to MRI including 52 malignant lesions and 38 benign lesions.

2.2 | CEDM and DBT

Mammography was performed using a Selenia mammography system (Hologic). An IV injection of 1.5 mL/kg body weight of a nonionic contrast medium (Visipaque 320; General Electric Healthcare, GE Healthcare, Inc) was carried out using a power injector with an injection rate of 2 mL/s.

After a 2-minute delay, the mammography technologist positioned the patient and compressed the breast as for a mammography examination in cranio-caudal (CC) and mediolateral oblique (MLO) view. For each breast, the CC view was collected first, followed 2 minute later by the MLO projection. The CEDM mode automatically collected 2 images in each view orientation: a low-energy acquisition at 26-30 kVp and a high-energy acquisition at 45-49 kVp, with kVp settings within those ranges depending on breast thickness and density.

Moreover, eight minutes after starting the contrast agent administration, the patient was positioned for a later mammographic examination in MLO view that includes low-energy and high-energy exposures and tomosynthesis. For each low- and high-energy pair, a weighted subtraction was performed automatically, generating an image that maximized the conspicuity of iodine contrast agent uptake.

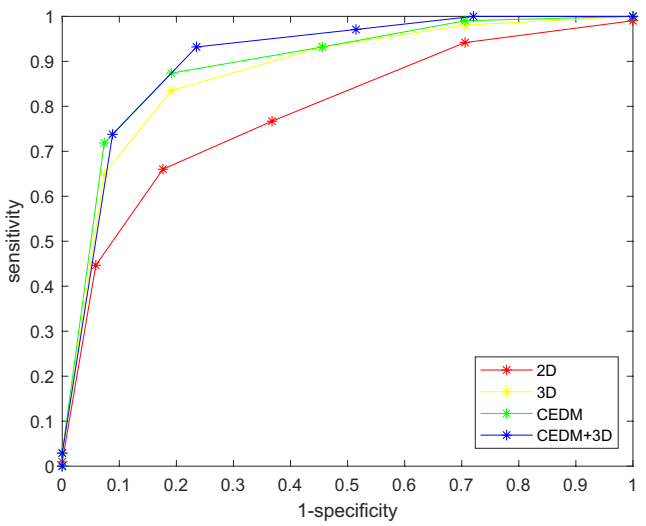

FIGURE 1 ROC curves for 2D, 3D, CEDM, and CEDM combined with 3D [Color figure can be viewed at wileyonlinelibrary.com]

2.3 | Magnetic resonance imaging

MRI was performed at 1.5 T (Magnetom Symphony, Siemens Medical Solutions) using a bilateral synchronous dedicated 16-channel breast coil. The patient was in the prone position. Examinations were scheduled on the 7th-14th days of the menstrual cycle in premenopausal women, but without scheduling limitations in postmenopausal women.

The technical MRI protocol included the following sequences:

1. Three-plane gradient-echo scout view.
2. Axial T1-weighted fat-saturated fast spin-echo (TR/TE = 564/12 ms; flip angle 90°; field of view 350 mm; acquisition matrix 512 × 512; pixel size 0.68 × 0.68 mm^2; slice thickness 2 mm; interslice gap 0 mm; acquisition time 4 minutes 12 seconds).
3. Axial T2-weighted short time inversion recovery (TR/TE/TI: 4000/56/160 ms; flip angle 180°; field of view 340 mm; acquisition matrix: 384 × 384; pixel size 0.89 × 0.89 mm^2; slice thickness 2 mm; interslice gap 0 mm; acquisition time 4 minutes 16 seconds).
4. Dynamic T1-weighted coronal three-dimensional fast low angle shot (FLASH) spoiled gradient-echo (TR/TE: 9.8/4.76 ms; flip angle 25°; field of view 370 × 185 mm^2; acquisition matrix 256 × 128; pixel size 1.45 × 1.45 mm^2; partition thickness 2 mm; interslice gap 0 mm; acquisition time 56 seconds).
5. Contrast-enhanced axial T1-weighted sequence equal to point 2.

The dynamic study consisted of one unenhanced and nine contrast-enhanced sequences. Contrast medium (Gd-DOTA, Guerbet)

TABLE 3 Diagnostic performance of 2D, 3D, CEDM, and CEDM combined to 3D

	AUC	Sensitivity	Specificity	PPV	NPV	Accuracy	*P* value
2D BIRADS	0.764	0.646	0.796	0.808	0.629	0.711	.045
DBT BIRADS	0.845	0.800	0.816	0.852	0.755	0.807	.038
CEDM BIRADS	0.879	0.815	0.796	0.841	0.765	0.807	.036
CEDM + 3D BIRADS	0.890	0.892	0.735	0.817	0.837	0.825	.037
CE-MRI BIRADS	0.892	0.908	0.837	0.881	0.872	0.877	.035
DCE-MRI BIRADS	0.934	0.954	0.878	0.912	0.935	0.921	.035

was injected at a standard single dose of 0.1 mmol/kg body weight at a flow rate of 2 mL/s, followed by 20 mL of saline solution at the same rate, using an automatic power injector (Spectris Solaris, Medrad).

Subtracted images (contrast-enhanced minus unenhanced images) were obtained for all dynamic phases. Dynamic curves of percent enhancement versus time were obtained for lesions at small regions of interest, positioned on the brightest portion of the lesion. Multiplanar reconstructions and maximum intensity projections of subtracted images were obtained when necessary.

2.4 | Image interpretation

Two-dimensional synthetized mammograms, CEDM, DBT, and MRI were evaluated in consensus by two experts among eight radiologists with at least 15 years of experience in breast imaging. Radiologists were blinded to final histopathological diagnosis; moreover, they were blinded to results of other techniques when evaluating the other techniques. The Breast Imaging Reporting and Data System (BIRADS) categorical scoring system[25] was used to analyze images. CE-MRI and DCE-MRI (CE-MRI including the information of time-intensity curve (TIC) type) were considered separately.

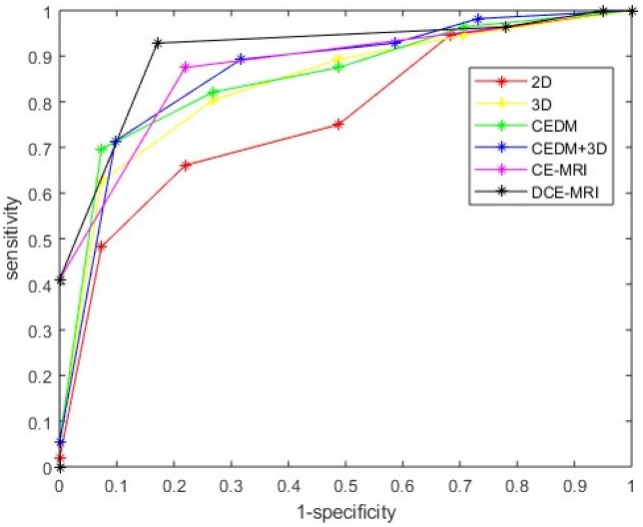

FIGURE 2 ROC curves for 2D, 3D, CEDM, CEDM combined with 3D, and MRI [Color figure can be viewed at wileyonlinelibrary.com]

2.5 | Reference standard and pathologic methods

The reference standard was pathology from surgical specimen for malignant lesions and pathology from surgical specimen or core needle biopsy for benign lesions. Tumor and nodal stage were classified according to the system implemented by the American Joint Committee on Cancer staging. The intensity, extent, and subcellular distribution of estrogen receptor (ER), progesterone receptor (PR), human epidermal growth factor receptor 2 (HER2), and Ki67 were evaluated as previously described.[26] The cutoff used to distinguish positive from negative cases was ≥1% for ER/PR ratio. Scores of 0 or 1+ were considered negative for HER2 expression, and 2+ and 3+ scores were positive. The percentage of positive cells per case for proliferative index Ki67 was scored according to 2 different groups: group 1, <15% (low proliferative activity, negative cases) and group 2, ≥15% (high proliferative activity, positive cases). Ductal carcinoma in situ and invasive cancers tumors were counted as malignant lesions. All other results, including lobular carcinoma in situ, fibroadenoma, ductal hyperplasia, dysplasia, cysts, and phyllodes tumor, were considered nonmalignant lesions.

2.6 | Statistical analysis

Continuous variables were reported as median and standard deviation value. Receiver operating characteristic (ROC) analysis was used. Area under ROC (AUC), sensitivity, specificity, positive predictive value (PPV), negative predictive value (NPV), and accuracy were calculated for 2D synthetized MX, CEDM, DBT (3D), CEDM combined to 3D, CE-MRI, and DCE-MRI. For intergroup comparisons, we used the Mann-Whitney *U* test for continuous variables and chi-square test for categorical variables. McNemar test was used to compare the diagnostic performance in terms of sensitivity and specificity. Spearman's or Pearson correlation coefficient was also calculated to compare BIRADS score of each imaging modality with pathologic findings and to compare lesions size reported by imaging modality respect to pathologic size. A P value < .05 was considered as significant. Calculations were performed using the Statistics and Machine Learning Toolbox of MATLAB R2007a (MathWorks).

TABLE 4 Diagnostic performance of 2D, 3D, CEDM, CEDM combined to 3D, CE-MRI, and DCE-MRI

	2D BIRADS	3D BIRADS	CEDM BIRADS	CE-MRI BIRADS	DCE-MRI BIRADS	TIC type	GRADING	ER	PgR	Ki_67	HERCEPTEST
2D BIRADS											
Correlation coefficient	1.000	0.757**	0.629**	0.447**	0.465**	0.442**	0.332**	0.290**	0.273**	0.345**	0.292**
P value		.000	.000	.000	.000	.000	.000	.001	.002	.000	.001
3D BIRADS											
Correlation coefficient	0.757**	1.000	0.844**	0.613**	0.627**	0.584**	**0.517****	0.425**	0.398**	0.493**	0.295**
P value	.000		.000	.000	.000	.000	.000	.000	.000	.000	.001
CEDM BIRADS											
Correlation coefficient	0.629**	0.844**	1.000	0.661**	0.661**	0.618**	**0.581****	0.437**	0.420**	**0.534****	0.360**
P value	.000	.000		.000	.000	.000	.000	.000	.000	.000	.000
CE-MRI BIRADS											
Correlation coefficient	0.447**	0.613**	0.661**	1.000	0.958**	0.849**	**0.608****	0.448**	0.404**	**0.514****	0.291**
P value	.000	.000	.000		.000	.000	.000	.000	.000	.000	.005
DCE-MRI BIRADS											
Correlation coefficient	0.465**	0.627**	0.661**	0.958**	1.000	0.894**	**0.633****	0.471**	0.427**	**0.541****	0.323**
P value	.000	.000	.000	.000		.000	.000	.000	.000	.000	.002
TIC type											
Correlation coefficient	0.442**	0.584**	0.618**	0.849**	0.894**	1.000	**0.639****	**0.546****	0.493**	0.**517****	0.337**
P value	.000	.000	.000	.000	.000		.000	.000	.000	.000	.001
GRADING											
Correlation coefficient	0.332**	0.517**	0.581**	0.608**	0.633**	0.639**	1.000	0.398**	0.389**	0.519**	0.316**
P value	.000	.000	.000	.000	.000	.000		.000	.000	.000	.000
ER											
Correlation coefficient	0.290**	0.425**	0.437**	0.448**	0.471**	0.546**	0.398**	1.000	0.958**	0.670**	0.489**
P value	.001	.000	.000	.000	.000	.000	.000		.000	.000	.000
PgR											
Correlation coefficient	0.273**	0.398**	0.420**	0.404**	0.427**	0.493**	0.389**	0.958**	1.000	0.641**	0.508**
P value	.002	.000	.000	.000	.000	.000	.000	.000		.000	.000
Ki_67											
Correlation coefficient	0.345**	0.493**	0.534**	0.514**	0.541**	0.517**	0.519**	0.670**	0.641**	1.000	0.631**
P value	.000	.000	.000	.000	.000	.000	.000	.000	.000		.000
HERCEPTEST											
Correlation coefficient	0.292**	0.295**	0.360**	0.291**	0.323**	0.337**	0.316**	0.489**	0.508**	0.631**	1.000
P value	.001	.001	.000	.005	.002	.001	.000	.000	.000	.000	

**Correlation significant with a *P* value < .01.

*Correlation significant with a *P* value < .05.

TABLE 5 Spearman correlation coefficients table among BIRADS score assessed by imaging and histopathological values

	CEDM size	3D size	MRI size	PATHOLOGIC size
CEDM size				
Correlation coefficient	1.000	0.912**	0.822**	0.722**
P value		.000	.000	.000
3D size				
Correlation coefficient	0.9129**	1.000	0.693**	0.684**
P value	.000		0.000	.000
MRI size				
Correlation coefficient	0.822**	0.693**	1.000	0.811**
P value	.000	.000		.000
Pathologic size				
Correlation coefficient	0.722**	0.684**	0.811**	1.000
P value	.000	.000	.000	

**Correlation significant with a *P* value < .01.

*Correlation significant with a *P* value < .05.

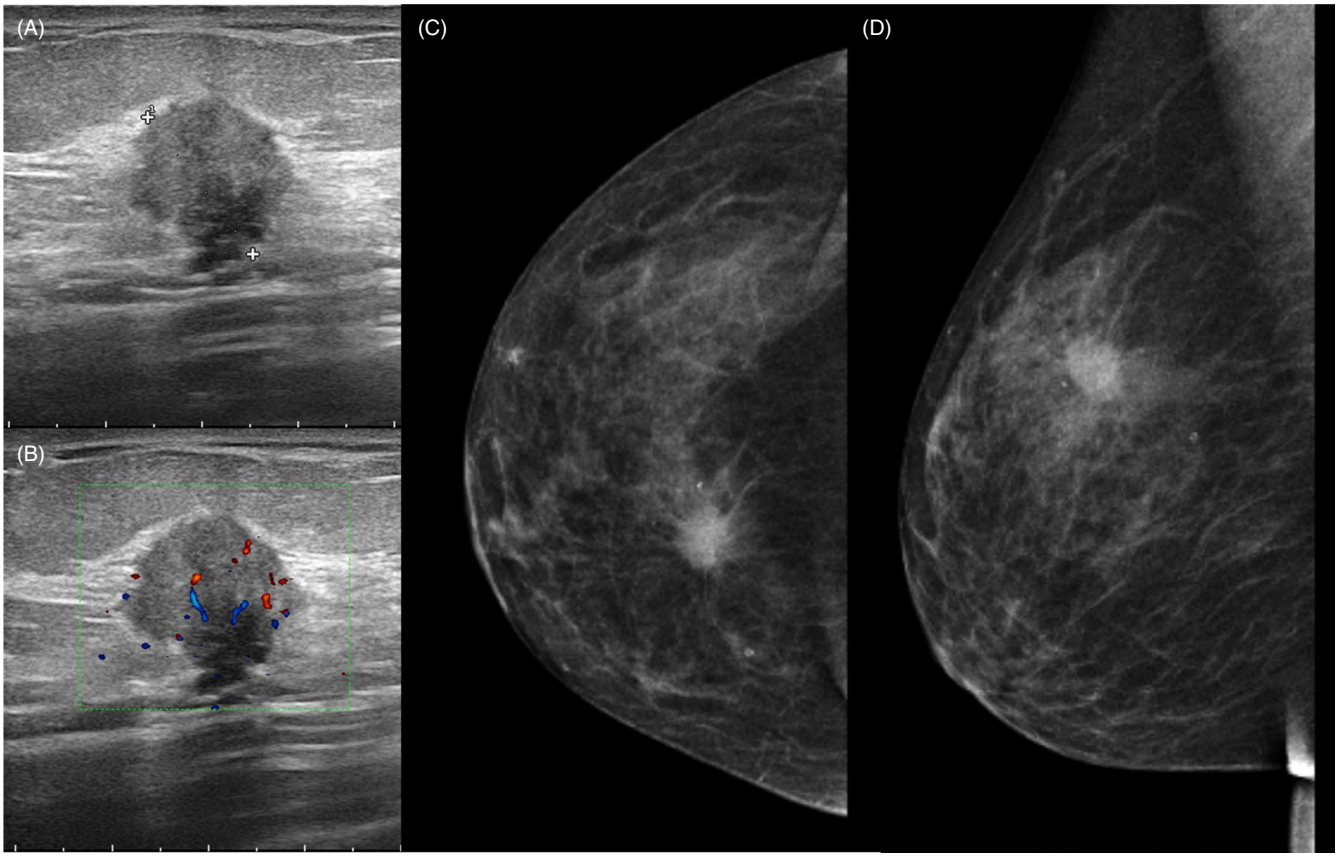

FIGURE 3 Right breast ultrasound (A). Vertically oriented, 15-mm nodule with irregular borders. Color Doppler (B). Multiple, irregular vessels inside the nodule. Digital synthetized MX, cranio-caudal (C) and oblique (D) view of the right breast. Adipose breast. Inner upper quadrant nodule with infiltrating borders. Histological diagnosis: invasive ductal carcinoma [Color figure can be viewed at wileyonlinelibrary.com]

3 | RESULTS

Table 2 reports the diagnostic performance of 2D, 3D, CEDM, and CEDM combined to 3D (see Figure 1). Table 3 reports the diagnostic performance of each modality including CE-MRI and DCE-MRI in a smaller group of patients (see Figure 2). Considering the latter group, 2D synthetized mammography showed an area under ROC curve (AUC) of 0.764 (sensitivity 65%, specificity 80%), while AUC was of 0.845 (sensitivity 80%, specificity 82%) for DBT, of 0.879 (sensitivity 82%, specificity 80%) for CEDM, and

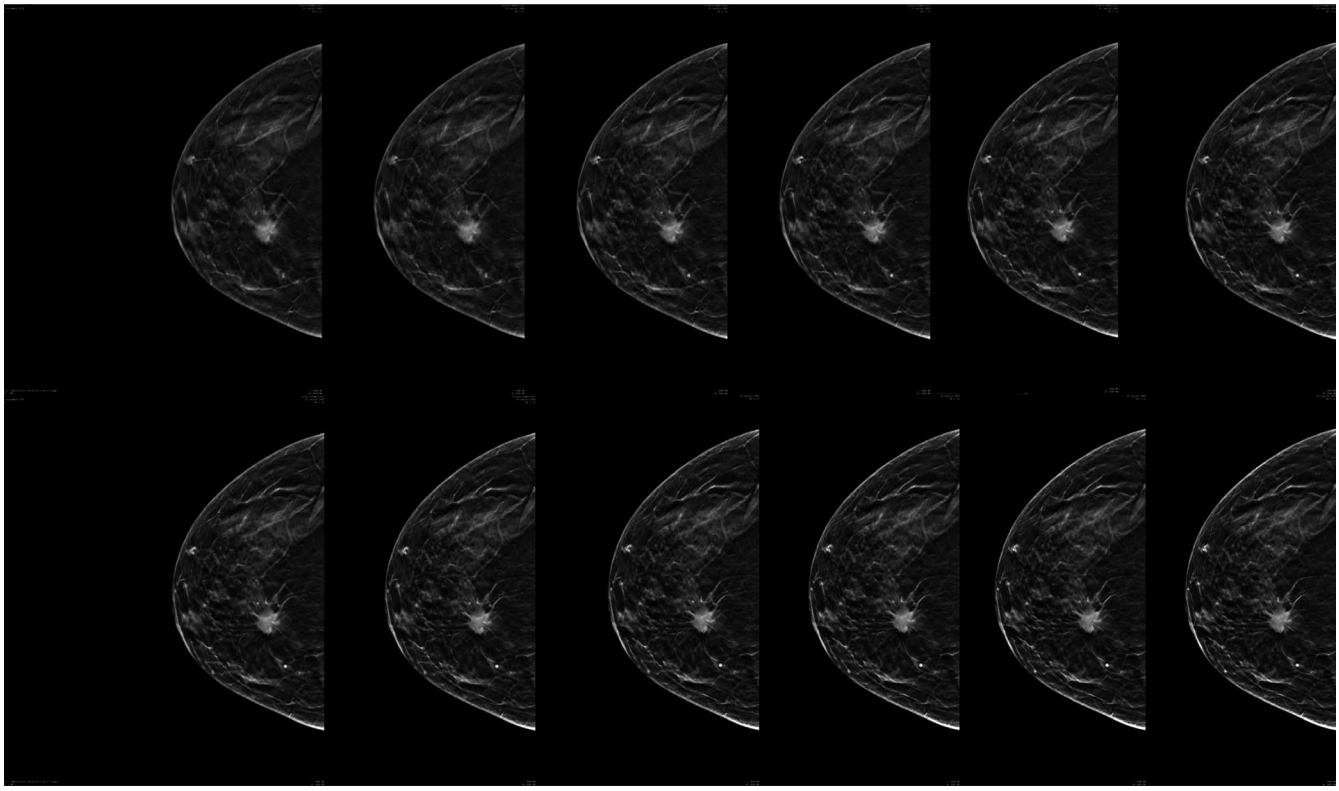

FIGURE 4 The same patient of Figure 3. Right breast DBT. Cranio-caudal sequence. Optimal depiction of the nodular formation, with spicules radiating in the surrounding tissue

FIGURE 5 The same patient of Figures 3 and 4. Right breast CEDM. Cranio-caudal (A) and oblique (B, C) images. Strong and homogeneous enhancement of the nodule. Right breast DCE-MRI. Intensely and homogeneously enhancing nodule (D and F). Quick wash-in TICs (E) [Color figure can be viewed at wileyonlinelibrary.com]

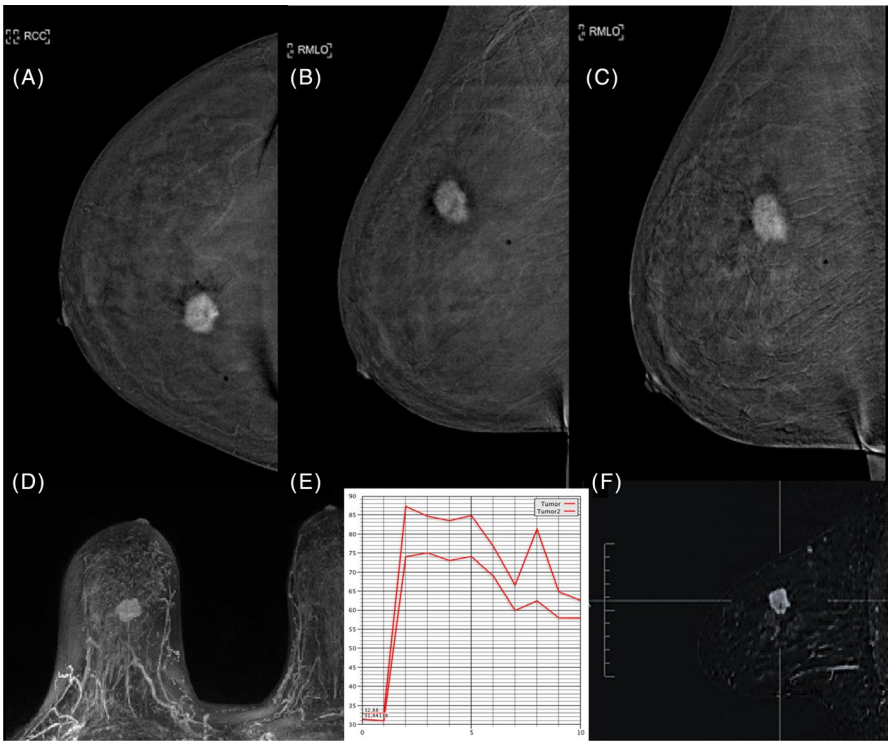

of 0.892 (sensitivity 91%, specificity 84%) for CE-MRI. DCE-MRI determined an AUC of 0.934 (sensitivity 96%, specificity 88%). Combined CEDM with 3D findings, we obtained an AUC of 0.890 (sensitivity 89%, specificity 74%).

The results were all statistically significant with a *P* value < .05 (Fisher exact test). DBT, CEDM, CE-MRI, and CEDM combined to DBT showed comparable diagnostic performance without a significant statistical difference in sensitivity and specificity value

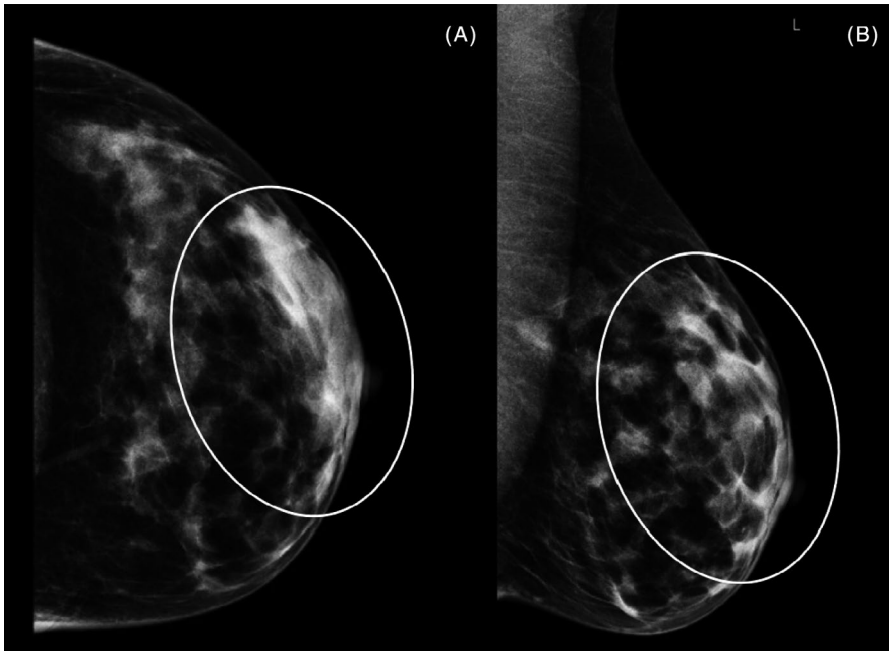

FIGURE 6 Digital synthetized MX, cranio-caudal (A) and oblique (B) view of the left breast. Nodular formation with irregular margins, around 2-cm large, in the upper-external quadrant. Histological diagnosis: multifocal invasive ductal carcinoma

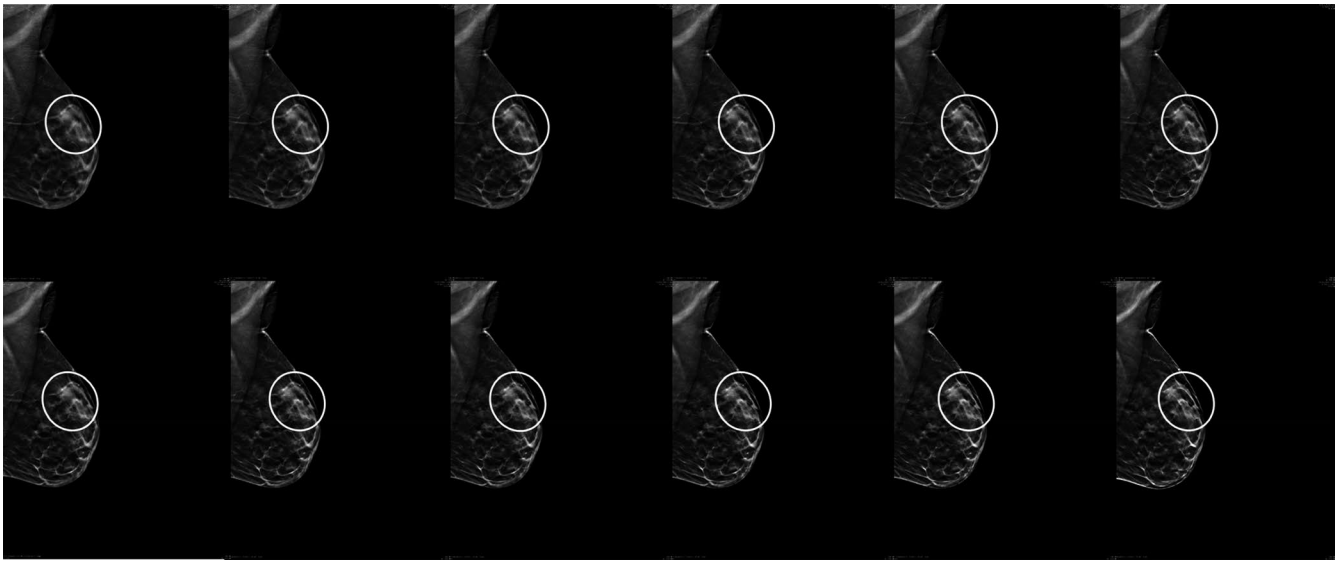

FIGURE 7 The same patient of Figure 5. Left breast DBT. Irregular formation, around 2-cm large, in the upper-external quadrant

(P > .05 at McNemar test), while a difference statistically significant was observed between DCE-MRI and CEDM (P = .03 at McNemar test).

A significant correlation (Table 4) was found between 3D BIRADS (r = .517), CEDM BIRADS (r = .581), CE-MRI BIRADS (r = .608), DCE-MRI BIRADS (r = .633), TIC type (r = .639), and grading. A significant correlation was found between CEDM BIRADS (r = .534), CE-MRI BIRADS (r = .514), DCE-MRI BIRADS (r = .541), TIC type (r = .517), and Ki-67 values. Only TIC type shows a significant correlation with ER and PgR values (r = .546 and 0.493, respectively).

Moreover, 3D, CEDM, CEDM combined to tomosynthesis, and DCE-MRI had a high ability to identify multifocal and bilateral lesions with a detection rate of 77% (26/34), 85% (29/34), 91% (31/34), and 95% (19/20), respectively, while the 2D had a detection rate for multifocal lesions of 56% (19/34).

The best correlation (Table 5) between imaging lesion size and pathologic size was obtained by DCE-MRI (r = .811). However, also CEDM obtained a high Pearson correlation value (r = .722).

Figures 3-11 represent some among the significant illustrations of DBT, CEDM, and DCE-MRI images for three enrolled patients.

4 | DISCUSSION

Breast MRI is the most sensitive imaging technique for breast cancer detection and the most accurate for assessment of extent

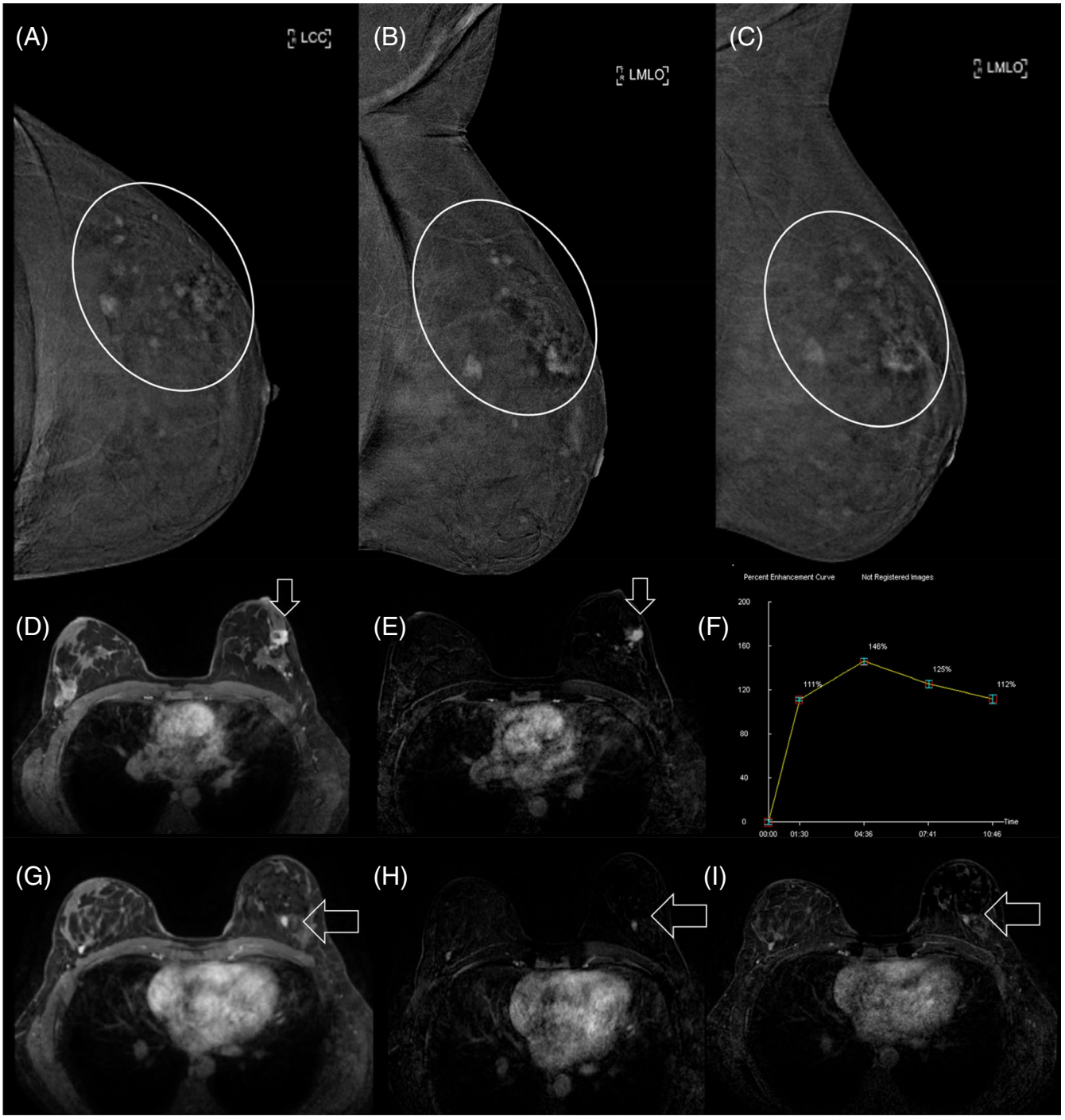

FIGURE 8 The same patient of Figures 5 and 6. Left breast CEDM. Cranio-caudal (A) and oblique (B, C) images. Multiple, enhancing tumor foci in the external upper quadrant. DCE-MRI. Multiple enhancing foci in the left breast (D, E, G, H, I). Rapid wash-in TIC with persistent enhancement (F) [Color figure can be viewed at wileyonlinelibrary.com]

of disease. However, breast MRI, cause the high-cost-benefit balance, its time consuming and its limited availability, is often used as a second step in a screening tool or in symptomatic women. DBT has been shown to provide exquisite information for mass, focal asymmetry, and architecture distortion with a significantly lower malignancy rate compared to 2D mammography.[27] CEDM is a promising imaging technique, which provides information from standard digital MX combined with enhancement characteristics related to underlying neoangiogenesis. Cheung et al[28] investigated the performance of CEDM versus MX in dense breasts. Their results suggested that using CEDM improves diagnosis by 21.2% in sensitivity, 16.1% in specificity, and 12.8% in overall accuracy. Tagliafico et al[27] recently summarized the diagnostic performance of CEDM in a systematic review of 8 eligible studies. The pooled sensitivity of CEDM was 98% (95% CI, 96%-100%), with a pooled specificity being moderate at 58% (95% CI, 38%-77%). Moreover,

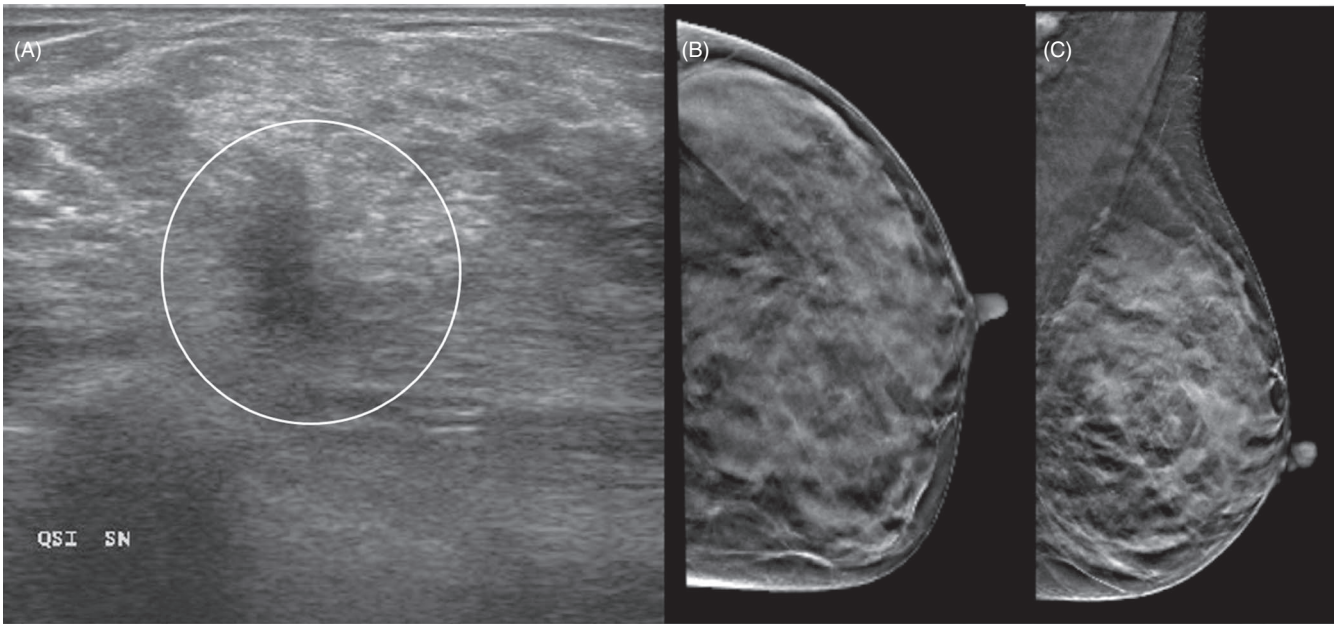

FIGURE 9 Left breast ultrasound, inner upper quadrant (A). Vertically oriented hypoechoic lesion, with infiltrating borders and dorsal attenuation. Digital MX, cranio-caudal (B) and oblique (C) view of the left breast. No definite lesion is evident within the moderately dense breast. Histological diagnosis: tubular infiltrating carcinoma associated with DCIS areas

CEDM is used for screening in women with an increased risk of breast cancer, showing a NPV of 99.7% and an increased cancer detection (by 75%) compared to the low-energy mammography, thanks to the addition of contrast enhancement.[28,29] Similar results are reported by Sorin et al.[30]

Some recent studies have concentrated on comparing CEDM with MRI. Fallenberg et al[22] imaged 80 subjects with newly diagnosed cancers and found that the sensitivity of CEDM was slightly better than that of MRI for the index lesion. Jochelson et al[23] studied 52 breast cancer women using MRI and CEDM. Both MRI and CEDM had better detection rate for index breast tumors than conventional mammography. Łuczyńska et al[31] suggested that CEDM has the potential to be a valuable diagnostic method that enables accurate detection of malignant breast lesions and has high negative predictive value and a false-positive rate similar to that of breast MRI.

In our current study, sensitivity was 100% for CEDM and 93% for MRI, and the accuracy was of 79% with CEDM and of 73% with breast MRI. ROC curve areas based on BIRADS were 0.83 for CEDM and 0.84 for MRI. Lesion size estimates on CEDM and MRI were similar, both slightly larger than those from histopathology.

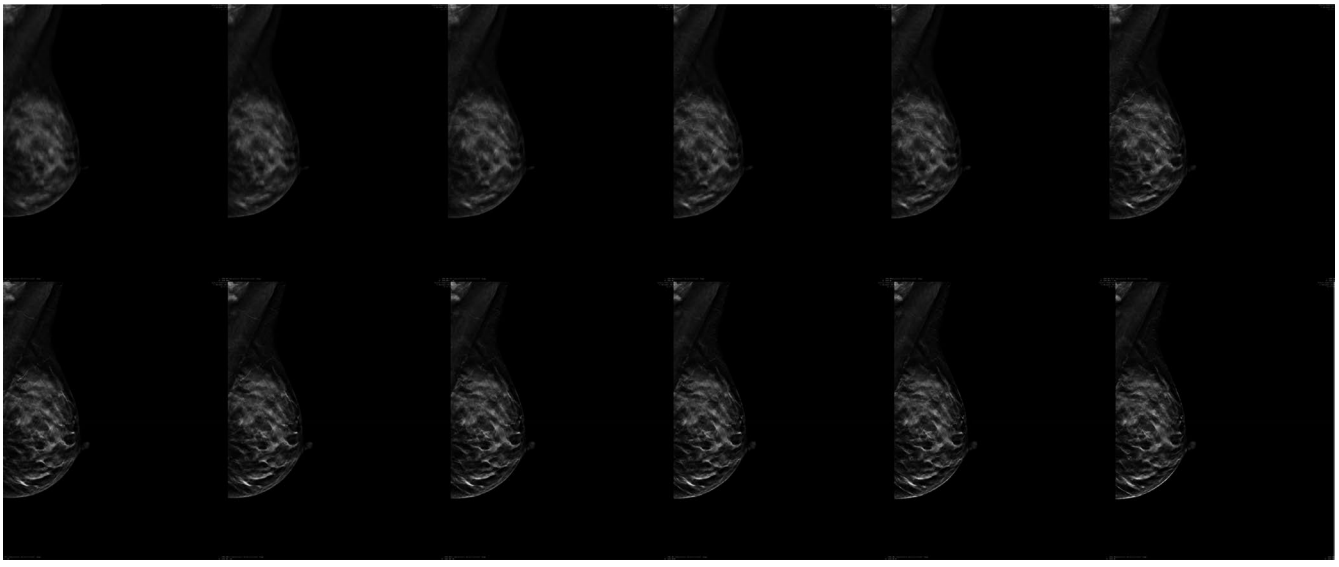

FIGURE 10 The same patient of Figure 9. Left breast DBT. No definite lesion is evident within the moderately dense breast

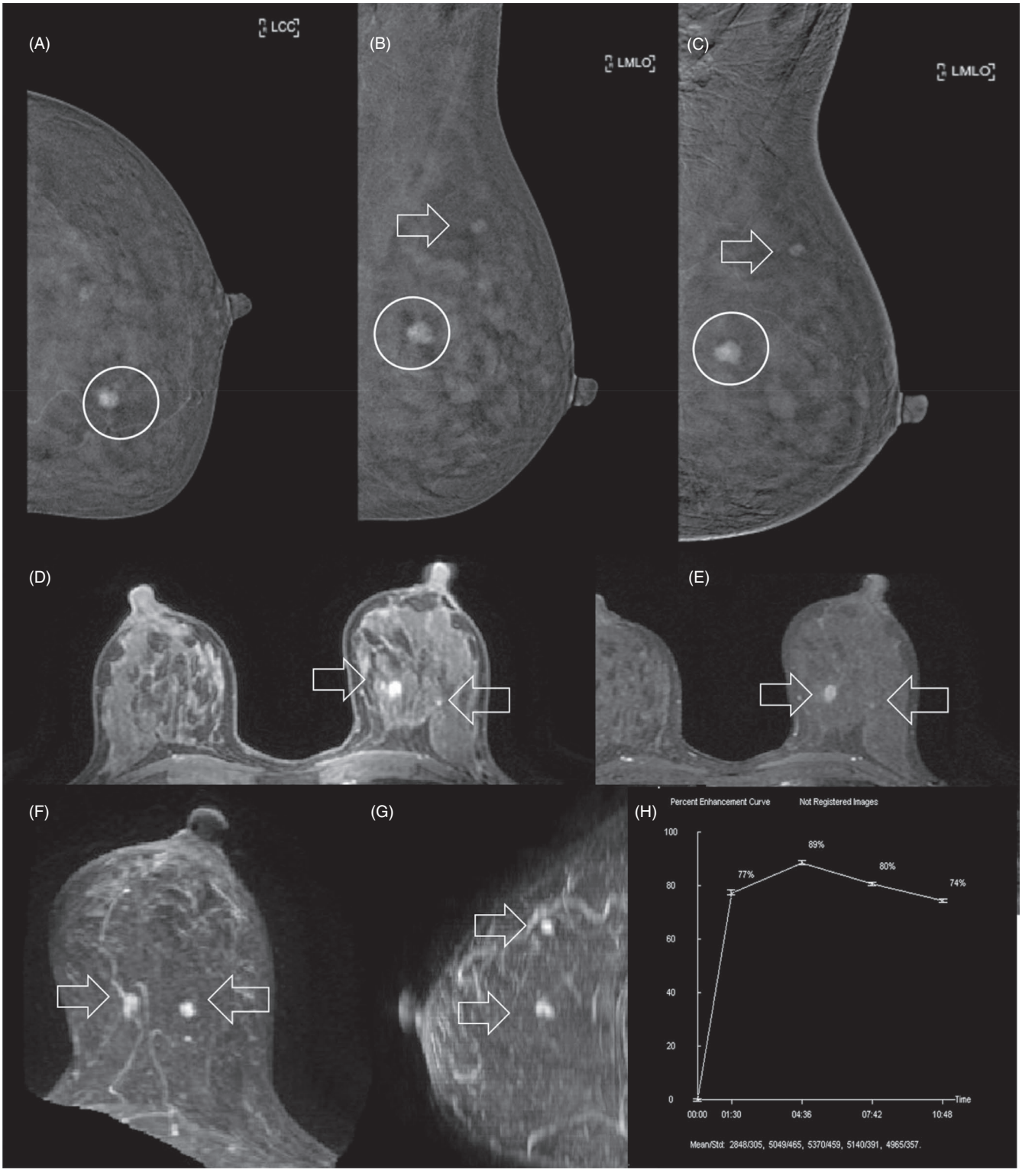

FIGURE 11 The same patient of Figures 9 and 10. Left breast CEDM. Cranio-caudal (A) and oblique (B, C) images. Two small enhancing tumor foci are visible. Left breast DCE-MRI. Two intensely enhancing tumor foci are visible (D-G). Quick wash-in TICs with persistent enhancement (H)

Our findings, comparable at recent literature results, demonstrated that both DBT and CEDM had an increase of accuracy compared to 2D synthetized mammography. Our results suggested that DBT improves diagnosis by 15% in sensitivity and 10% in overall accuracy compared to 2D alone and CEDM improves diagnosis by 17% in sensitivity and 10% in overall accuracy compared to 2D alone. We demonstrated that DBT, CEDM, CE-MRI, and CEDM combined to DBT had similar diagnostic performance without a significant statistical difference in sensitivity and specificity ($P > .05$ at McNemar test). Moreover, our finding shows that, like breast CE-MRI, CEDM combined with DBT (sensitivity of 91%)

could be of particular value for detection and assessment of extent of breast cancer having high sensitivity to detect breast lesions, to differentiate benign from malignant disease, and to assess multifocal breast lesions. A difference statistically significant was observed between DCE-MRI and CEDM. DCE-MRI improves diagnosis by 14% in sensitivity and 11% in overall accuracy compared to CEDM alone. Therefore, the dynamic information of DCE-MRI study by means of time-intensity curve type (curve with rapid wash-in and wash-out was considered to differentiate malignant lesion from benign lesion) has an important role to increase sensitivity and specificity in breast lesion detection. The dynamic functional information including entire phase of contrast agent uptake allows a better classification of benign and malignant breast lesions.

Our study findings are alike with those presented by Li et al[32]; these authors showed that both CEDM and MRI had high sensitivity for detection of breast cancer. Additionally, they reported that CEDM had a higher PPV than MRI and has the potential to play an important tool in breast cancer detection and staging. Instead, we found an higher value of PPV in DCE-MRI than in CEDM. Probably these differences are due to the different balancing between malignant and benign lesions of two studies. Li et al[32] study involved a total of 66 lesions including 62 malignant and 4 benign lesions without to perform the classification between malignant and benign lesions. In our study, we considered the ability of this classification and also the ability to assess breast cancer extension. We reported that although CEDM and CEDM combined to DBT had high detection rate to detect multifocal and bilateral lesions while DBT alone had a lower detection rate, DCE-MRI had the highest capability with a percentage detection value of 96%.

Moreover, we demonstrated that the best correlation between imaging lesion size and pathologic size was obtained by DCE-MRI (r = .811).

In the end, we reported that a significant correlation was found between DBT BIRADS, CEDM BIRADS, CE-MRI BIRADS, DCE-MRI BIRADS, TIC type, and grading. A significant correlation was found between CEDM BIRADS, CE-MRI BIRADS, DCE-MRI BIRADS, TIC type, and Ki-67 values, while only TIC type shows a significant correlation with ER and PgR values. As reported before, DBT can detect small breast cancer in a dense parenchyma reducing false-positive recall. Skaane at al report, as a result of their prospective study based on OTST, that the additional cancers detected with 2D + DBT compared to single 2D, in a screening tool, had molecular subtypes luminal A or Luminal B Her2 negative with a very low Ki67 expression characterized to have a very good prognosis. These finding raise the suspicion that some cancer should be "overdetected".[33] Therefore, it is important to keep in mind that "overdiagnosis," followed by "overtreatment," does not diminish the benefit of mammography in decreasing breast cancer mortality.[34] In a future prospective, the goal should not be the "overdiagnosis," but it should be the better treatment decision tool,[35] which is, maybe feasible, with a higher correlation between the histopathological characterization of the lesion and its contrast enhancement behavior on CE-MRI or CEDM.

The methodological limitations of the current study include the following: Readers' finding was obtained in consensus; a synthetized 2D image (or synthetic equivalent) was included as part of the tomosynthesis study, and therefore, the two modalities are not independent each other; another limitation of our study was that CEDM is a novel technique and consequently does not yet have a dedicated BIRADS lexicon and classification system; and as a result, we adopted rules described by Diekmann et al.[36]

In conclusions, DBT and CEDM have superior diagnostic accuracy of 2D synthetized MX to identify and classify breast lesions, and CEDM combined with DBT has better diagnostic performance compared with DBT alone. Moreover, the present study suggests that, like breast CE-MRI, CEDM combined with DBT could be of particular value for detection and assessment of extent of breast cancer having high sensitivity to detect breast lesions and to assess multifocal breast lesions. However, an increase of population size will need to investigate and verify it. The best results in terms of diagnostic performance were obtained by DCE-MRI. Dynamic information obtained by time-intensity curve including entire phase of contrast agent uptake allows a better detection and classification of breast lesions, but as already reported in literature, CEDM could be a supplemental imaging examination in women with an increased risk of breast cancer who do not meet MRI criteria or for whom access to MRI is limited.[37]

ACKNOWLEDGEMENTS

The authors are grateful to Alessandra Trocino, librarian at the National Cancer Institute of Naples, Italy.

CONFLICT OF INTEREST

Each author declares that there is no conflict of interest.

AUTHORS' CONTRIBUTIONS

AP conceived the study, participated in its design and coordination, and drafted the manuscript. RF and MS participated in the studies collection, analyzed the data, and drafted the manuscript. PV, OC, SF, VG, TP, MRR, SVS, FM, CR, CS, MDB, and GB participated in the studies collection. All authors read and approved the final manuscript.

ETHICAL APPROVAL

All procedures performed in studies involving human participants were in accordance with the ethical standards of the institutional and national research committee and with the 1964 Helsinki Declaration and its later amendments or comparable ethical standards. This study was approved by our local Institutional Review Board. Informed consent was obtained from all individual participants included in the study.

CONSENT TO PUBLISH

All patients provided informed consent for the use of their data for research purposes.

DATA AVAILABILITY STATEMENT

Data sharing is not applicable to this article as no data sets were generated or analyzed during the current study.

ORCID

Roberta Fusco https://orcid.org/0000-0002-0469-9969

REFERENCES

1. Emaus MJ, Bakker MF, Peeters PH, et al. MR Imaging as an additional screening modality for the detection of breast cancer in women aged 50–75 years with extremely dense breasts: the DENSE trial study design. *Radiology*. 2015;277(2):527-537.
2. Loberg M, Lousdal ML, Bretthauer M, Kalager M. Benefits and harms of mammography screening. *Breast Cancer Res*. 2015;17:63.
3. Lee EH, Kim KW, Kim YJ, et al. Performance of screening mammography: a report of the alliance for breast cancer screening in Korea. *Korean J Radiol*. 2016;17(4):489-496.
4. Sardanelli F, Podo F, D'Agnolo G, et al. Multicenter comparative multimodality surveillance of women at genetic-familial high risk for breast cancer (HIBCRIT study): interim results. *Radiology*. 2007;242(3):698-715.
5. Van Ongeval C, Van Steen A, Vande Putte G, et al. Does digital mammography in a decentralized breast cancer screening program lead to screening performance parameters comparable with film-screen mammography? *Eur Radiol*. 2010;20(10):2307-2314.
6. Autier P, Boniol M. Mammography screening: a major issue in medicine. *Eur J Cancer*. 2018;90:34-62.
7. Freer PE. Mammographic breast density: impact on breast cancer risk and implications for screening. *Radiographics*. 2015;35(2):302-315.
8. Gilbert FJ, Tucker L, Gillan MG, et al. Accuracy of digital breast tomosynthesis for depicting breast cancer subgroups in a UK retrospective reading study (TOMMY Trial). *Radiology*. 2015;277(3):697-706.
9. Skaane P, Bandos AI, Gullien R, et al. Comparison of digital mammography alone and digital mammography plus tomosynthesis in a population-based screening program. *Radiology*. 2013;267(1):47-56.
10. Ciatto S, Houssami N, Bernardi D, et al. Integration of 3D digital mammography with tomosynthesis for population breast-cancer screening (STORM): a prospective comparison study. *Lancet Oncol*. 2013;14(7):583-589.
11. Miglioretti DL, Abraham L, Lee CI, et al. Digital breast tomosynthesis: radiologist learning curve. *Radiology*. 2019;291(1):34-42.
12. Petrillo A, Fusco R, Petrillo M, et al. Added value of breast MRI for preoperative diagnosis of ductal carcinoma in situ: diagnostic performance on 362 patients. *Clin Breast Cancer*. 2017;17(3):e127-e134.
13. Petrillo A, Fusco R, Filice S, et al. Breast contrast enhanced MR imaging: semi-automatic detection of vascular map and predominant feeding vessel. *PLoS ONE*. 2016;11(8):e0161691.
14. Petrillo A, Porto A, Fusco R, et al. Surgical impact of preoperative breast MRI in women below 40 years of age. *Breast Cancer Res Treat*. 2013;140(3):527-533.
15. Esserman LJ, Kumar AS, Herrera AF, et al. Magnetic resonance imaging captures the biology of ductal carcinoma in situ. *J Clin Oncol*. 2006;24(28):4603-4610.
16. Houssami N, Hayes DF. Review of preoperative magnetic resonance imaging (MRI) in breast cancer: should MRI be performed on all women with newly diagnosed, early stage breast cancer? *CA Cancer J Clin*. 2009;59(5):290-302.
17. Van Goethem M, Verslegers I, Biltjes I, Parizel PM. MR is/is not a useful diagnostic tool for breast cancer management. *Acta Chir Belg*. 2007;107(3):267-270.
18. Hollingsworth AB, Stough RG, O'Dell CA, Brekke CE. Breast magnetic resonance imaging for preoperative locoregional staging. *Am J Surg*. 2008;196(3):389-397.
19. Mann RM, Veltman J, Barentsz JO, Wobbes T, Blickman JG, Boetes C. The value of MRI compared to mammography in the assessment of tumour extent in invasive lobular carcinoma of the breast. *Eur J Surg Oncol*. 2008;34(2):135-142.
20. Dromain C, Balleyguier C, Adler G, et al. Contrast-enhanced digital mammography. *Eur J Radiol*. 2009;69:34-42.
21. Dromain C, Thibault F, Muller S, Garbay JR, Delaloge S. Dual-energy contrast-enhanced digital mammography: initial clinical results. *Eur Radiol*. 2011;21:565-574.
22. Fallenberg EM, Dromain C, Diekmann F, Engelken F, Krohn M, Singh JM. Contrast-enhanced spectral mammography versus MRI: initial results in the detection of breast cancer and assessment of tumour size. *Eur Radiol*. 2014;24:256-264.
23. Jochelson MS, Dershaw DD, Sung JS, et al. Bilateral contrast-enhanced dual-energy digital mammography: feasibility and comparison with conventional digital mammography and MR imaging in women with known breast carcinoma. *Radiology*. 2013;266:743-751.
24. Badr S, Laurent N, Regis C, Boulanger L, Lemaille S, Poncelet E. Dual-energy contrast-enhanced digital mammography in routine clinical practice in 2013. *Diagn Interv Imaging*. 2014;95:245-258.
25. https://www.acr.org/Clinical-Resources/Reporting-and-Data-Systems/Bi-Rads
26. Alshafei TU, Nguyen JV, Rochman CM, Nicholson BT, Patrie JT, Harvey JA. Outcome of architectural distortion detected only at breast tomosynthesis versus 2D mammography. *Radiology*. 2018;288(1):38-46.
27. Tagliafico AS, Bignotti B, Rossi F, et al. Diagnostic performance of contrast-enhanced spectral mammography: systematic review and meta-analysis. *Breast*. 2016;28:13-19.
28. Cheung YC, Lin YC, Wan YL, et al. Diagnostic performance of dual-energy contrast-enhanced subtracted mammography in dense breasts compared to mammography alone: interobserver blind-reading analysis. *Eur Radiol*. 2014;24:2394-2403.
29. Sung JS, Lebron L, Keating D, et al. Performance of dual-energy contrast-enhanced digital mammography for screening women at increased risk of breast cancer. *Radiology*. 2019;293(1):81-88.
30. Sorin V, Yagil Y, Yosepovich A, et al. Contrast-enhanced spectral mammography in women with intermediate breast cancer risk and dense breasts. *AJR Am J Roentgenol*. 2018;211(5):W267-W274.
31. Łuczyńska E, Heinze-Paluchowska S, Hendrick E, et al. Comparison between breast MRI and contrast-enhanced spectral mammography. *Int Med J Exp Clin Res*. 2015;21:1358-1367.
32. Li L, Roth R, Germaine P, et al. Contrast-enhanced spectral mammography (CESM) versus breast magnetic resonance imaging (MRI): a retrospective comparison in 66 breast lesions. *Diagn Interv Imaging*. 2017;98(2):113-123.
33. Skaane P, Sebuødegård S, Bandos AI, et al. Performance of breast cancer screening using digital breast tomosynthesis: results from the prospective population-based Oslo Tomosynthesis Screening Trial. *Breast Cancer Res Treat*. 2018;169(3):489-496.
34. Yang TL, Liang HL, Chou CP, Huang JS, Pan HB. The adjunctive digital breast tomosynthesis in diagnosis of breast cancer. *Biomed Res Int*. 2013;2013:597253.
35. Hayse B, Hooley RJ, Killelea BK, Horowitz NR, Chagpar AB, Lannin DR. Breast cancer biology varies by method of detection and may contribute to overdiagnosis. *Surgery*. 2016;160(2):454-462.
36. Diekmann F, Freyer M, Diekmann S, et al. Evaluation of contrast-enhanced digital mammography. *Eur J Radiol*. 2011;78(1):112-121.
37. Jochelson MS, Pinker K, Dershaw DD, et al. Comparison of screening CEDM and MRI for women at increased risk for breast cancer: a pilot study. *Eur J Radiol*. 2017;97:37-43.

How to cite this article: Petrillo A, Fusco R, Vallone P, et al. Digital breast tomosynthesis and contrast-enhanced dual-energy digital mammography alone and in combination compared to 2D digital synthetized mammography and MR imaging in breast cancer detection and classification. *Breast J*. 2019;00:1–13. https://doi.org/10.1111/tbj.13739